Developmental Biology 494 (2023) 35–45

Contents lists available at ScienceDirect

Developmental Biology

journal homepage: www.elsevier.com/locate/developmentalbiology

FGF signalling is involved in cumulus migration in the common house spider *Parasteatoda tepidariorum*

Ruixun Wang [a], Daniel J. Leite [b], Linda Karadas [a], Philipp H. Schiffer [a], Matthias Pechmann [a,*]

[a] Institute for Zoology/Developmental Biology, Biocenter, University of Cologne, Zuelpicher Str. 47b, 50674, Cologne, Germany
[b] Department of Biosciences, Durham University, Durham, DH1 3LE, UK

ARTICLE INFO

Keywords:
Cell migration
Spider
Cumulus
DV axis
FGF
Hedgehog
BMP
Ets4

ABSTRACT

Cell migration is a fundamental component during the development of most multicellular organisms. In the early spider embryo, the collective migration of signalling cells, known as the cumulus, is required to set the dorsoventral body axis.

Here, we show that FGF signalling plays an important role during cumulus migration in the spider *Parasteatoda tepidariorum*. Spider embryos with reduced FGF signalling show reduced or absent cumulus migration and display dorsoventral patterning defects. Our study reveals that the transcription factor *Ets4* regulates the expression of several FGF signalling components in the cumulus. In conjunction with a previous study, we show that the expression of *fgf8* in the germ-disc is regulated via the Hedgehog signalling pathway. We also demonstrate that FGF signalling influences the BMP signalling pathway activity in the region around cumulus cells.

Finally, we show that FGFR signalling might also influence cumulus migration in basally branching spiders and we propose that *fgf8* might act as a chemo-attractant to guide cumulus cells towards the future dorsal pole of the spider embryo.

1. Introduction

In vertebrates, like mice and humans, almost two dozen of ligands and four receptors are responsible for the regulation of one of the most complex signalling pathways, the Fibroblast-Growth-Factor-Receptor (FGFR) signalling pathway. Differential splicing of the receptors and different ligand/receptor combinations are able to regulate a wealth of biological processes including axis establishment, cell proliferation, differentiation and survival (reviewed in (Dorey and Amaya, 2010; Xie et al., 2020)). In contrast to vertebrates, the genomes of invertebrates such as beetles or flies only have a handful of fibroblast growth factor receptors and ligands ((Beermann and Schröder, 2008; Sharma et al., 2015, 2013) and reviewed in (Muha and Müller, 2013)). Nevertheless, in these animals FGFR signalling is also involved in a variety of important developmental processes, such as the formation of the mesoderm and the branching of the tracheal system (summarized in (Muha and Müller, 2013; Sharma et al., 2015)). In *Drosophila*, these two processes involve the regulation of directed cell migration, another widely conserved feature of the FGFR-signalling pathway. By acting as chemo-attractants, FGFs are able to attract cells by altering components of the cytoskeleton, which in turn leads to the formation of filo- and lammellipodia (e.g. (Clark et al., 2011; Sato and Kornberg, 2002), reviewed in (Muha and Müller, 2013)).

In the nematode *Caenorhabditis elegans*, EGL-15 and EGL-17 (the FGF receptor and FGF orthologs of *C. elegans*) are involved in a chemo-attractive mechanism to guide sex myoblasts to their final destination (Borland et al., 2001; Burdine et al., 1998; Lo et al., 2010).

Furthermore, in vertebrates FGFR signalling controls cell migration in various tissues. In mouse embryos, endoderm- and mesoderm-derived tissues depend on the outward migration of cells from the primitive streak, and this process is controlled by a small subset of FGFs (Sun et al., 1999).

Setting up the dorsoventral (DV) body axis of chelicerate species, like spiders, involves the migration of the cumulus (a cluster of cells that possesses organizing capacities). Cumulus cells are inducing the DV body axis via the secretion of Dpp (the BMP2/4 ortholog) and the subsequent activation of the BMP signalling pathway in a subset of germ-disc cells (Akiyama-Oda and Oda, 2003, 2006; Hilbrant et al., 2012; Oda and Akiyama-Oda, 2008; Pechmann, 2020; Pechmann et al., 2017; Schwager et al., 2015). As the name implies, the germ-disc is radially symmetric and gives rise to the embryo proper. Cumulus transplantation or the local activation of the BMP signalling pathway demonstrated that all germ-disc

* Corresponding author.
E-mail address: pechmanm@uni-koeln.de (M. Pechmann).

https://doi.org/10.1016/j.ydbio.2022.11.009
Received 24 March 2022; Received in revised form 28 November 2022; Accepted 30 November 2022
Available online 5 December 2022

cells have the capacity to develop either into ectodermal embryonic or into dorsal field cells (Holm, 1952; Oda et al., 2020; Pechmann, 2020). For this reason, the decision if a germ-disc changes its fate towards a dorsal field cell depends on the signalling and the direction of cumulus migration.

It is still unclear if the direction of cumulus migration in the radially symmetric field of germ-disc cells is actively guided via unknown factors, or if cumulus migration is a completely stochastic process. Hedgehog signalling was found to play a role in cumulus migration (Akiyama-Oda and Oda, 2010, 2020). However, it is unknown if Hedgehog is directly or indirectly involved during this important developmental process.

Here we show that cumulus migration in the common-house spider *Parasteatoda tepidariorum* is highly dependent on FGFR signalling. We show that a FGF ligand is asymmetrically expressed in the early germ-disc of many spider embryos and we suggest that FGFR signalling is involved in the guidance of the cumulus cells towards the periphery of the germ-disc.

2. Methods

2.1. Spider husbandry and embryology

For all experiments we used our Cologne laboratory culture of *P. tepidariorum*. Adults and juveniles of *P. tepidariorum* were kept in plastic vials at room temperature and were fed with *Drosophila melanogaster* and crickets (*Gryllus bimaculatus*). Embryos were collected and fixed as described previously (Pechmann et al., 2017) and staged according to (Mittmann and Wolff, 2012). *Acanthoscurria geniculata* embryos were kept as described previously (Pechmann, 2020). Adults and juveniles of *Steatoda grossa* were collected near Cologne (Hürth, Germany) and were kept under the same conditions as *P. tepidariorum*.

2.2. Gene cloning

CLC Main Workbench 7 (QIAGEN Aarhus A/S) was used to perform a local tBLASTn (Altschul et al., 1990) against the *P. tepidariorum* official AUGUSTUS gene set (https://i5k.nal.usda.gov/Parasteatoda_tepidariorum (Schwager et al., 2017)). For this, protein sequences of known homology were downloaded from FlyBase (Thurmond et al., 2019) and NCBI. Putatively identified genes were reciprocally BLASTed against the online NCBI nr database using BLASTx to confirm their identity.

PCR amplification and cloning of genes was performed using standard techniques. Genes were cloned into the pCR4 and the pCRII vector (ThermoFisher scientific). *Pt-Ets4*, *Pt-fork-head*, *Pt-orthodenticle*, *Pt-short-gastrulation*, *Pt-decapentaplegic*, *Pt-hedgehog* and *Pt-caudal* were isolated previously (McGregor et al., 2008; Pechmann et al., 2009, 2017).

A *Pt-fgf8* DNA fragment of approximately 2 kb, including the full coding sequence and a portion of the 5′UTR and the 3′UTR, was amplified using Pt-fgf8-Fw (5′-CATCTCTTCGCTCTCCGCGC-3′) and Pt-fgf8-Rev (5′-GAATGCTCGTGCAAAGAGAGTG-3′).

Pt-dof, Pt-fgf1, Pt-FGFR1 and *Pt-FGFR2* were amplified using Pt-dof–Fw (5′-GAAATGGCTCCTGTCGACGTTAC-3′), Pt-dof–Rev (5′-CAATACTGGAACAGGTTGAGCTG-3′), Pt-fgf1-Fw (5′-GTGGATAGAGGCATACCGAGT-3′), Pt-fgf1-Rev (5′-CGGAACACCTCTACGGAACG-3′), Pt-FGFR1-Fw (5′-GACATATGCTGAGGAAGATAATAG-3′), Pt-FGFR1-Rev (5′-CAAACGTTATTTGAATCTGAATC-3′), Pt-FGFR2-Fw (5′-GTCACAGTCATTTTAGGCTTG-3′) and Pt-FGFR2-Rev (5′-CAGTGTACATCTCCTGAGGTAC-3′) primer, respectively.

The *P. tepidariorum fgf1* and *fgf8* sequences were BLAST queried to the published transcriptome of *A. geniculata* (Pechmann, 2020) to identify *A. geniculata fgf1*, *fgf8* and *fgf17* sequences. Total RNA was isolated and cDNA was produced as described in (Pechmann, 2020). *Ag-fgf* gene sequences were isolated using the following primer combinations: Ag-fgf1-Fw (5′-GTG CAA CGA GGA CAA CTA TTC AG-3′) and Ag-fgf1-Rev (5′-GAG TAC TAT ACA TTT CAA AAC ACC G-3′); Ag-fgf8-Fw (5′-CTC CAT GCT TCA CCG TTG ATG-3′) and Ag-fgf8-Rev (5′-CTG CTG TCA TTG GCA CTT GTC-3′); Ag-fgf17-Fw (5′-GAA CAG CCT GAG CAA ATG CCA C-3′) and Ag-fgf17-Rev (5′-CAC CTG AGA ATC TTG CTG GAC AC-3′).

Nucleotide sequences of *fgf8* and *fgf17* of different spider species were blasted against the combined RNA-Seq from 19 Libraries sequenced from the false black widow (*S. grossa*) (SRR1539523). Blast hits were manually aligned and primer sequences of *S. grossa fgf8* and *fgf17* were designed according to this alignment. Total RNA of *S. grossa* was extracted using TRIzol Reagent (life technologies) and cDNA was produced using the RNA to cDNA EcoDry Premix (TaKaRa Clontec, double primed). *Sg-fgf8* and *Sg-fgf17* were amplified using Sg-fgf8-Fw (5′-CAG GTT ACT ACA GAT TGC CTC C-3′) and Sg-fgf8-Rev (5′-GTA CGT GTG CTC CCT CTT GAT G-3′) and Sg-fgf17-Fw (5′-GTT CAT CTG CAC TTC TGT CAT GG-3′) and Sg-fgf17-Rev (5′-CCG TGT GTC ATT CCA GAG ATG-3′) primer, respectively.

2.3. Parental RNAi experiments

For parental RNAi (pRNAi) adult spider females were injected 3–4 times (in a 2–3 day interval) with 2 μl [2–3 μg/μl] dsRNA solution. *Pt-ptc* and *Pt-Ets4* pRNAi experiments were performed as described in (Pechmann et al., 2017). Double stranded RNA was produced using the T7 MEGAscript Kit (ThermoFisher scientific).

During the initial pRNAi screen *Pt-fgf8* (AUGUSTUS prediction: aug3.g5611.t1 (Schwager et al., 2017)) was amplified using the g5611-Fw (5′-CAGGTTACTACAGATTGCCTCC-3′) and g5611-Rev (5′-GCACTTTCGTTCGTATTCATAG-3′) primer. To generate the dsRNA, the template was amplified using the T7 overhang primer T7-g5611-Fw (5′-GTAATACGACTCACTATAGGGCTAGCGTACCTGTGT-3′) and T7-g5611-Rev (5′-GTAATACGACTCACTATAGGGGCCAGTCCCCAGC-3′). Two non-overlapping DNA fragments coding for *Pt-fgf8* were amplified using T7-Pt-fgf8-off1-Fw (5′-GTAATACGACTCACTATAGGGCTCCGCGCTGCGGC-3′) and T7-Pt-fgf8-off1-Rev (5′-GTAATACGACTCACTATAGGGCGCCTCAATAGTGGAGC-3′) and T7-Pt-fgf8-off2-Fw (5′-GTAATACGACTCACTATAGGGGTGTGTCTATTCAAAGAAGG-3′) and T7-Pt-fgf8-off2-Rev (5′-GTAATACGACTCACTATAGGGGGATGATGAGAGATCTATAG -3′), respectively. These DNA fragments were used as a template to generate dsRNA that targeted independent regions of the *Pt-fgf8* transcript. For the metrics shown in Fig. 1C, four spider females were injected with dsRNA of each *Pt-fgf8* fragment, respectively. The metrics shown for *Pt-dof* (Fig. 1C) is based on three injected spider females.

Pt-hh was cloned into pCRII vector using Pt-hh-Fw (5′-GGTACACCCATAAATGCCGTCAGTTGAG-3′) and Pt-hh-Rev (5′-GTATATTCATGACAAGCGCCAGATCACACC-3′). Subsequently, T7 and T7M13R primer were used to generate the template for dsRNA production. Several spiders were injected with the generated *Pt-hh* dsRNA and only severely affected cocoons were used for the experiments shown in this study.

2.4. Transcriptome sequencing of cumulus cells

To knock down *Pt-Ets4*, several spider females were injected with *Pt-Ets4* dsRNA constructs from nucleotides 11–697 of aug3.g4238.t1 and dsRed for negative control injections as described in (Pechmann et al., 2017). For each cocoon approximately 50 embryos were monitored under Halocarbon 700 (Merck) oil to observe developmental phenotypes. From each spider injection, stage 4 control and *Pt-Ets4* RNAi embryos of 3rd and 4th cocoons were formaldehyde fixed and stored in 100% MeOH at −20°C. Subsequently, the cumulus was extracted using sharp needles from fixed stage 4 embryos from control and *Pt-Ets4* knockdowns (see (Pechmann et al., 2017)). The cumulus of 100–120 embryos was extracted for each replicate. For each condition (control vs. *Ets4* pRNAi) the embryos from three cocoons from three independent injections were used. Overall, three biological and technical replicates were produced per condition. The total RNA of the extracted cells was isolated using the Quick-RNA™ FFPE Kit (Zymo Research). Library preparation and

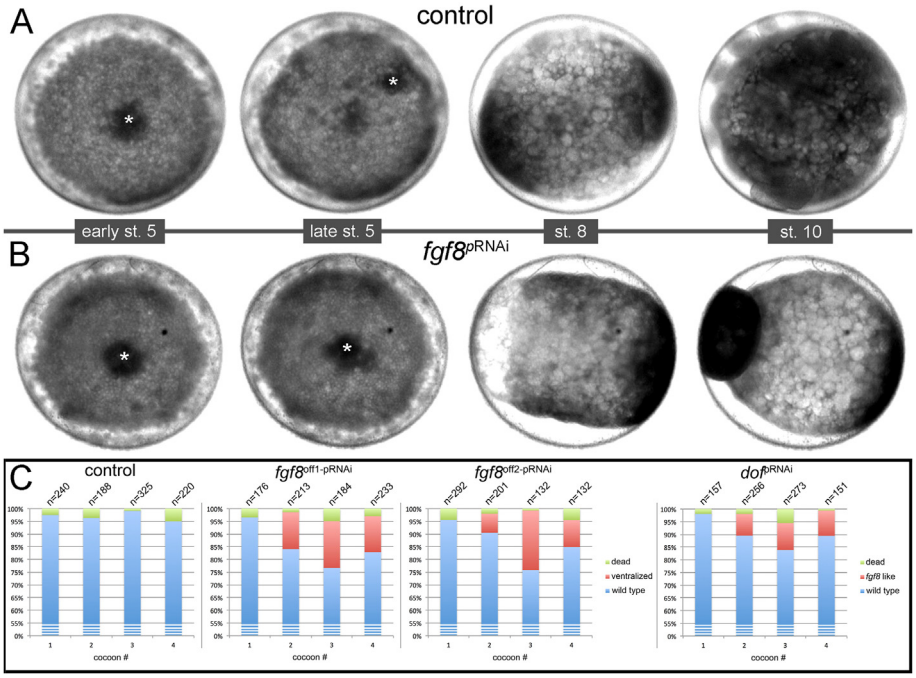

Fig. 1. Knockdown of *Pt-fgf8* prevented cumulus migration. (**A**, **B**) Stills from Movie S1. In contrast to the control embryo, the cumulus (marked by the asterisk in **A** and **B**) of the *Pt-fgf8* knockdown embryo is not shifting and stays in the centre of the germ-disc during stage 5 of embryonic development. The *Pt-fgf8* knockdown embryo was radially symmetric and showed a tube-like morphology during later stages of development (st. 8 - st. 10). (**C**) Efficiency of the *Pt-fgf8* and *Pt-dof* knockdown. To check for "off-target" effects, four spider females were injected with dsRNA of two non-overlapping *Pt-fgf8* fragments (off1 and off2), each. Embryos were monitored under oil. Similar to the knockdown of *Pt-fgf8*, also the knockdown of the downstream factor *Pt-dof* resulted in knockdown embryos that displayed the typical tube-like (*fgf8*-like) phenotype.

sequencing was carried out at the Cologne Center for Genomics, using a paired-end 2 × 150nt approach on the Illimuna NovaSeq platform. The sequenced reads were subjected to adaptor and quality threshold trimming using fastp (Chen et al., 2018). Cleaned reads where mapped against the published *P. tepidariorum* gene set (Schwager et al., 2017) using kallisto (Bray et al., 2016) and the expression metrics were analysed in Degust (David Powell (2015), drpowell/degust v3.2.0 (v3.2.0); Zenodo; https://doi.org/10.5281/zenodo.3258933).

2.5. Phylogenetic analysis

The FGF core sequence (see (Beermann and Schröder, 2008)) was used to align FGF proteins of different species. In case of Dof related proteins, only the conserved DBB (Dof, BCAP, BANK region) motif as well as the region of the ankyrin repeats were used to generate the phylogeny. Alignments were produced using MUSCLE (Edgar, 2004) and aligned sequences were trimmed using TrimAl with the GappyOut setting (Capella-Gutiérrez et al., 2009). Maximum likelihood based phylogenies were constructed using PhyML at 'phylogeny.fr' (Dereeper et al., 2008). Final phylogenies were generated with the WAG substitution model and 1000 bootstrap replicates (Whelan and Goldman, 2001). Gene bank accession numbers or sequences can be found in the supplemental information (figure legends of Figs. S1 and S5 and Supplemental Sequences).

2.6. Synteny analysis of FGF genes in spider genomes

To identify the synteny relationships of *FGF* genes in spiders we surveyed several high contiguity spider genomes. We used the three entelegynae species *P. tepidariorum* (Schwager et al., 2017), *Trichonephila antipodiana* (Fan et al., 2021), *Argiope bruennichi* (Sheffer et al., 2021) and the haplogynae species *Dysdera silvatica* (Escuer et al., 2022). FGF sequences for *fgf1*, *fgf8 fgf17* and *dof* from the phylogenetic analysis, were used to Diamond blastp (Buchfink et al., 2021) query the genome annotations and confirmed through reciprocal blasts to NCBI. Nucleotide and protein sequences are given in Supplemental Sequences. Genomic locations were extracted from GTFs. MCScanX (Wang et al., 2012) with default settings was also used to attain further synteny relationships between species' scaffolds that contained FGFs. A custom python script transformed each gene location from syntenic clusters in the MCScanX collinearity file into minimum and maximum coordinates for each cluster. Gene locations and synteny relationships (as ribbon links) were plotted with Circos (Krzywinski et al., 2009).

2.7. Embryo fixation, in situ hybridisation and pMad antibody staining

To analyse BMP pathway activity in control and *Pt-fgf8* knockdown embryos a pMad antibody staining was performed as described in (Pechmann et al., 2017). Fluorescent pMad antibody staining was performed using the Phospho-Smad1/5 (Ser463/465) (41D10) Rabbit mAb (Cell Signaling Technology, Inc.; antibody concentration: 1:1000) as primary and an Alexa488 anti rabbit AB (Invitrogen; 1:400 concentration) as secondary antibody.

2.8. In situ hybridisation

In situ hybridisation was performed as described previously (Pechmann et al., 2017; Prpic et al., 2008). Fluorescent *in situ* hybridisation was performed using FastRed (Benton et al., 2016). Double *in situ* hybridisation was performed using NBT/BCIP and INT/BCIP as a substrate.

2.9. Imaging and image analysis

Embryos were imaged using an Axio Zoom.V16 that was equipped with an AxioCam 506 color camera. Confocal imaging was performed on a LSM 700 (Zeiss). Projections of image stacks were carried out using Helicon Focus (HeliconSoft) or Fiji (Schindelin et al., 2012). Live imaging was carried out on the Axio Zoom.V16 and images were processed using Fiji. Living embryos were monitored under Voltalef H10S or Halocarbon 700 (Merck) oil and live imaging was performed at RT.

Movies were created using Fiji. Images have been adjusted for brightness and contrast using Adobe Photoshop CS5.1.

False-colour overlays of *in situ* hybridization images were generated as described in (Pechmann et al., 2017).

3. Results

3.1. Cumulus migration requires FGF signalling

A previous pRNAi screen, designed to find new genes that are involved in the process of axis specification in *P. tepidariorum* revealed that the transcription factor *Pt-Ets4* has an important role during axis formation in spiders (see (Pechmann et al., 2017)). During this studies pRNAi screen the knockdown of a gene, orthologous to *fgf8* (named *Pt-fgf8* in this study; AUGUSTUS genome prediction: aug3.g5611.t1; see Fig. S1), also led to a strong defective dorsoventral axis patterning phenotype in a portion of *P. tepidariorum* embryos.

Phylogenomic interrogation of fibroblast growth factor like proteins revealed that the *P. tepidariorum* genome possesses two genes that code for FGF ligands (Fig. S1). This contrasts with many other spider species where we could find three FGFs. Phylogenetic analysis revealed that spider FGFs fall into the FGF A and D families (FGF families according to (Popovici et al., 2005), see Fig. S1). All analysed spider species have a clear homolog for Fgf1 and Fgf8. In addition, most spider genomes/-transcriptomes contain a homolog for *fgf17*, which seems to be missing in *Parasteatoda* as well as in *Trichonephila* (see Figs. S1 and S2). The wealth of genomic as well as transcriptomic resources that are available for *P. tepidariorum* (Posnien et al., 2014; Schwager et al., 2017), in addition to the chromosome level assembly that is available for the genome of *T. antipodiana* (Fan et al., 2021) indicates, that *fgf17* was lost independently in multiple spider lineages. Analysing the synteny relationships of FGFs in spiders with chromosome level assembled genomes reveals that FGFs are located on different chromosomes in *A. brunnichi* as well as in *T. antipodiana* (Fig. S2). Only in the haplogyne spider *D. sylvatica fgf-1* and *fgf-17* are located on the same chromosome. As a high contiguity spider genome is missing for *P. tepidariorum*, we failed to analyse synteny relationships of FGFs in this spider species (see Fig. S2).

Time lapse imaging of *Pt-fgf8* knockdown embryos revealed that the down regulation of *Pt-fgf8* prevented cumulus migration at stage 5 of development (Fig. 1, Movie S1). In control embryos, morphogenetic processes lead to the opening of the germ-disc and to the formation of the bilaterally symmetric germ-band embryo resulting in a clear dorsoventral polarity (Fig. 1A; Movie S1). This was in contrast to *Pt-fgf8* pRNAi embryos in which germ-disc opening and dorsal field formation did not occur. As a result, the knockdown embryos had a tube-like morphology at germ-band stages (Fig. 1B; Fig. 2B, Movie S1, Movie S2).

Supplementary data related to this article can be found at https://doi.org/10.1016/j.ydbio.2022.11.009.

As already mentioned, only a portion of the *Pt-fgf8* pRNAi embryos showed a DV patterning phenotype in the initial knockdown experiment. In this initial knockdown experiment almost the complete coding sequence of *Pt-fgf8* was used to generate dsRNA for pRNAi injections. To verify and quantify this observation and to rule out that this low knockdown efficiency was fragment specific, we tested two non-overlapping fragments spanning the complete coding sequence (see Fig. 1C; $fgf8^{off1-pRNAi}$) as well as a large region of the 3′UTR of *Pt-fgf8* (see Fig. 1C; $fgf8^{off2-pRNAi}$). For both dsRNA fragments we observed a very similar number of tube-like embryos at germ-band stages. By analysing the embryos of the second, third and fourth cocoon that were produced by the injected females, on average, 15,7% and 13,8% of tube-like embryos were observed for the two dsRNA fragments, respectively. With 18,5% (for fragment $fgf8^{off1}$) and 23,5% (for fragment $fgf8^{off2}$) the highest number of affected embryos were present in the third cocoon (around 3 weeks after injection, see Fig. 1C).

To overcome the low knockdown efficiency, we searched for other components of the FGF signalling pathway. Scanning the *P. tepidariorum* genome (Schwager et al., 2017), we found two paralogous genes coding for FGF receptors (named *Pt-FGFR1* (aug3.g26565.t1) and *Pt-FGFR2* (aug3.g26271.t1) in this study) and an ortholog of a gene known as *downstream-of-fgf* (*dof*), *stumps* (*sms*) or *heartbroken* (*hbr*) (named *Pt-dof* in this study; aug3.g4286.t1). We analysed the expression of the genes and found that *Pt-FGFR1* and *Pt-dof* were expressed in the migrating cumulus of stage 5 embryos, while *Pt-FGFR2* did not show any expression at germ-disc stage (Figs. S3–S5).

As expected from previous analysis (Akiyama-Oda and Oda, 2010) the knockdown of the two *fgf* receptors did not lead to any detectable defect in cumulus migration. In contrast, 11,3% (affected embryos of cocoon #3; see Fig. 1C) of the *Pt-dof* RNAi embryos showed a phenotype that was identical to the phenotype observed for the knockdown of *Pt-fgf8* (Fig. S5I). However, as the *Pt-dof* knockdown did not result in a higher frequency of tube-like phenotypes, we used the *Pt-fgf8* pRNAi

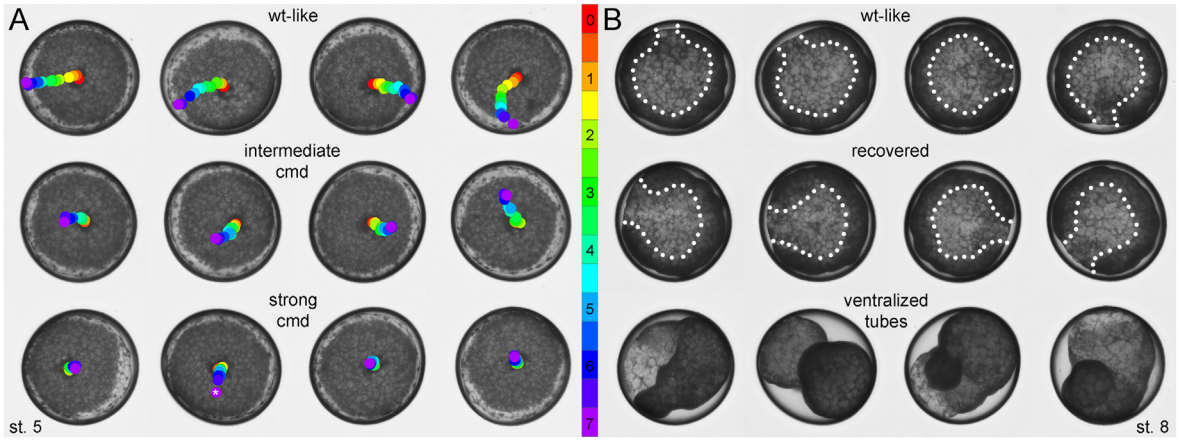

Fig. 2. Analysis of cumulus migration defects in *Pt-fgf8* knockdown embryos. Stills from Movie S2 at early stage 5 (**A**) and late stage 8 (**B**). Depicted is a selection of embryos taken from the 4th cocoon of a female that was injected with *Pt-fgf8* dsRNA. The colored dots indicate the initial (red), intermediate (orange to blue), and final (magenta) position of the cumulus during its migration from early to late stage 5. In embryos that showed a wt-like cumulus shift (wt-like, embryos of the upper row), the cumulus reached the rim of the germ-disc within a six to seven hour time window (compare to (Akiyama-Oda and Oda, 2010), the value of the numbers displayed in the color code is given in hours). Time-laps imaging revealed that embryos with intermediate cumulus-migration-defects (cmd) were able to quickly recover from the initial (at stage 6/7), tube-like phenotype (compare to Movie S2). At stage 8, the embryos that were showing a wt-like as well as an intermediate cumulus migration defect phenotype were virtually identical and had a wt-like morphology. In contrast, *Pt-fgf8* pRNAi embryos showing a strong cumulus migration defect phenotype (embryos depicted in the lower row) retained their radially symmetry and developed into ventralized tubes. The asterisk indicates a shift in the position of the cumulus that is due to the movement of the embryo within the perivitelline space (compare to Movie S2 and S3). White dots in **B** outline the dorsal rim of the germ-bands that grew around the inner yolk mass.

embryos for further analyses.

A close analysis via time laps imaging and cumulus tracking of *Pt-fgf8* pRNAi embryos of a strongly affected *Pt-fgf8* pRNAi cocoon, revealed that in 37% (n = 65) of the analysed embryos, the cumulus shifted towards the rim of the germ-disc within a six to seven hour time window (see embryos in the upper row of Fig. 2A, Movie S2 and S3). This cumulus migration behaviour can be regarded as wild type-like (wt-like), as it is similar to what was observed for embryos that were obtained from a control *gfp* pRNAi experiment (Akiyama-Oda and Oda, 2010). Embryos that showed a wt-like migration behaviour at stage 5 also showed a wt-like embryonic development that included dorsal-field and germ-band formation (see embryos in the upper row of Fig. 2A and Movie S2). However, in 12% and 28% of the analysed embryos the cumulus showed an intermediate (middle row of embryos shown in Fig. 2A and Movies S2 and S3) or strong (lower row of embryos shown in Fig. 2A and Movies S2 and S3) cumulus migration defect phenotype, respectively. In this experiment, the cumulus of embryos showing strong cumulus migration defects, arrested in the centre of the germ-disc throughout stage 5. In contrast, the cumulus of embryos showing an intermediate cumulus migration defect was able to shift around half the distance towards the rim of the disc, during the seven hour time window. Interestingly, all of the embryos that showed an intermediate cumulus migration defect were only transiently radially symmetric at stages 6–7 and were able to recover and formed virtually wt-like germ-bands at stage 8. 33% (n = 18) of the embryos showing a strong cumulus migration defect developed the tube-like phenotype, while the remaining embryos were able to re-establish a DV body axis and showed a wt-like morphology at later stages of development (Fig. 2; Movie S2). The remarkable ability of spider embryos to recover from a strong DV patterning defect and to re-establish a new DV body axis has already been noted before (Pechmann et al., 2017).

Supplementary data related to this article can be found at https://doi.org/10.1016/j.ydbio.2022.11.009.

As revealed by an *in situ* hybridisation for the ventral cell fate marker *short gastrulation* (*Pt-sog*) and the anterior marker *orthodenticle* (*Pt-otd*), stage 8 *Pt-fgf8* knockdown embryos were completely ventralized and were lacking any bilateral symmetry (Fig. 3A–E). However, the staining of *Pt-otd* at the anterior and *caudal* (*Pt-cad*) at the posterior pole indicated that anterior and posterior patterning was not affected by the knockdown of *Pt-fgf8* (Fig. 3D–G).

In conclusion, the knockdown of *Pt-fgf8* as well as of the downstream effector *Pt-dof* prevented cumulus migration in the spider *P. tepidariorum*. As cumulus migration is required for the formation of the dorsoventral body axis, FGF signalling is a necessary regulator during early spider embryogenesis.

3.2. Stochastic germ-disc expression of *Pt-fgf8*

It is known that FGF ligands can function as a chemo attractant to cells that express a FGF receptor (reviewed in e.g. (Muha and Müller, 2013)). For this reason, we were interested to see whether *Pt-fgf8* might be expressed in a subset of germ-disc cells to be able to guide the *Pt-FGFR1* expressing cumulus cells towards the rim of the germ-disc.

At stage 3 and 4, *Pt-fgf8* transcripts were detected within the central primary thickening of the germ-disc (Fig. 4A–C). Confocal sectioning of stage 4 embryos revealed that fluorescently labelled *Pt-fgf8* transcripts were present in the gastrulating cells that entered the germ-disc via the blastopore (see Fig. 4C).

Single cells or groups of ectodermal germ-disc cells started to express *Pt-fgf8* (Fig. 4B', Fig. 4C) at the beginning of stage 4. At the end of stage 4 (Fig. 4D–E, Fig. S6) many embryos showed a clear asymmetric *Pt-fgf8* expression. In extreme cases, half of the germ-disc was positive while the other half was mostly negative for *Pt-fgf8* transcripts (Fig. 4E, Figs. S6A, C, E, F, I). However, at stage 4 every embryo showed a unique pattern and the expression of *Pt-fgf8* was very variable. While in some embryos *Pt-fgf8* could be detected in only a few germ-disc cells (e.g. Figs. S6B and G) other embryos showed a nearly ubiquitous expression of *Pt-fgf8* (e.g. Figs. S6D and H). At late-stage 4, expression was switched off from the primary thickening and was restricted to the ectodermal cells of the germ-disc (e.g. Fig. 4D; e.g. Figs. S6B and G, J).

A similar stochastic and variable expression of *Pt-fgf8* was also detected at early and mid-stage 5 embryos when the cumulus cells started

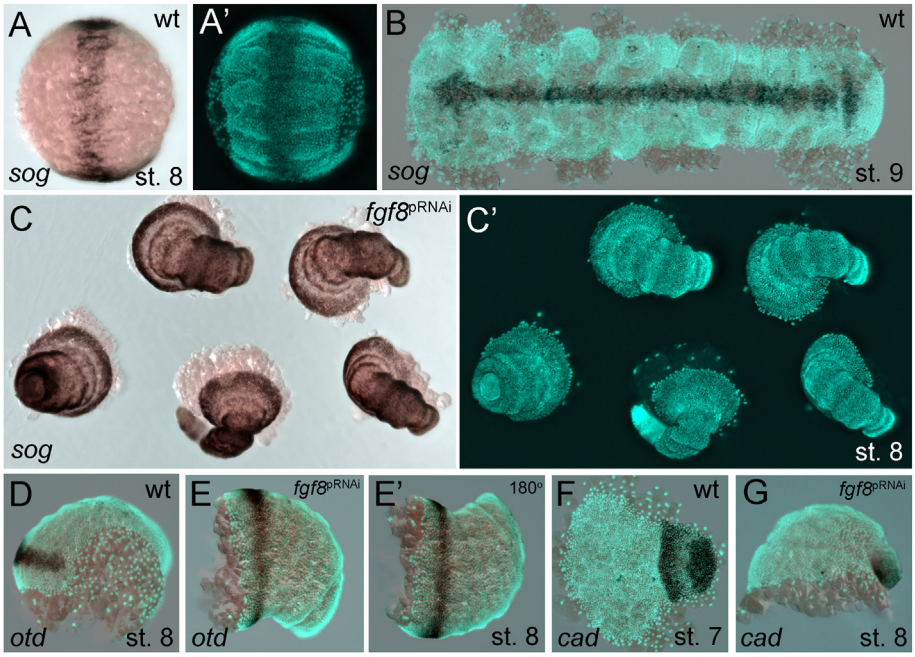

Fig. 3. *Pt-fgf8* knockdown embryos were radially symmetric, ventralized and displayed a tube-like morphology. (**A-G**) Expression of a ventral (*Pt-sog*), an anterior (*Pt-otd*) and a posterior (*Pt-cad*) marker gene in control and *Pt-fgf8* knockdown embryos. Whole mounted (**A**, **C**, **D**, **E**, **G**) and flat mounted (**B**, **F**) embryos co-stained with the nuclear dye Sytox green. To clearly show the radially symmetry, the embryo shown in **E** was turned by 180° (**E'**).

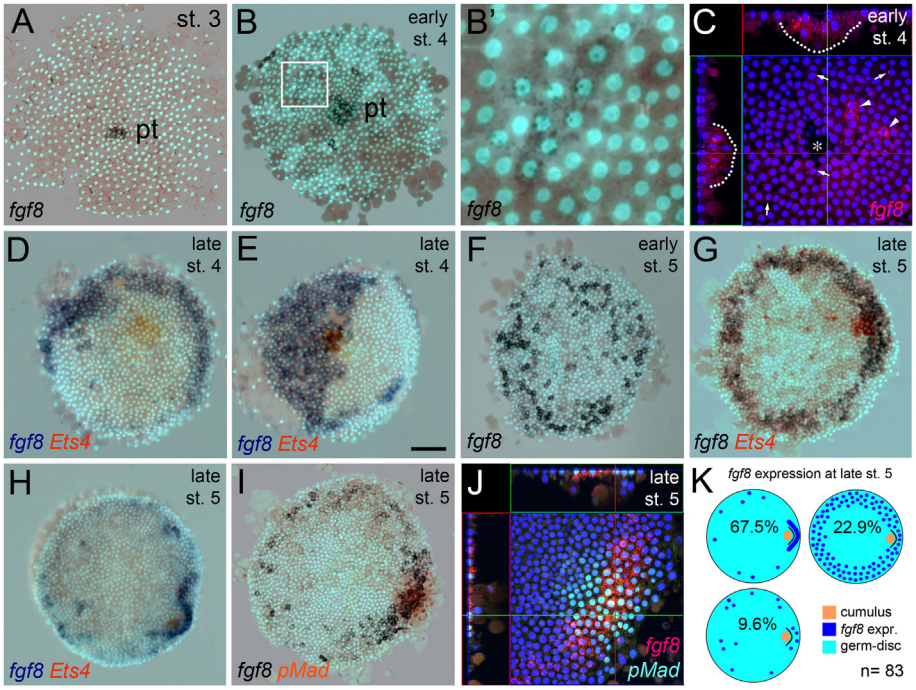

Fig. 4. Stochastic expression of *Pt-fgf8* in the germ-disc. (**A-C**) At stage 3 and 4, cells delaminate via the blastopore (see asterisk in **C**) and form the primary thickening (pt in **A** and **B**). The cells of the primary thickening were positive for *Pt-fgf-8* transcripts (outlined by the dotted line in the orthogonal views in **C**). At early stage 4, *Pt-fgf8* was stochastically activated in single or in groups of cells within the ectoderm of the germ-disc (see boxed region in **B** and arrows and arrow heads in **C**). Nascent transcripts in the nuclei (arrow heads) and cells with *Pt-fgf8* transcripts in the cytoplasm (arrows) of the germ-disc cells are indicated in **C**. Boxed region in **B** is magnified in **B'**. (**D, E**) Two embryos that showed an extreme asymmetric localisation of *Pt-fgf8* transcripts within the germ-disc at late-stage 4. (**F, G**) Two examples for a spotted (**F**) or ring-like (**G**) expression of *Pt-fgf8* transcripts at early and late-stage 5. (**G-K**) At late-stage 5, most embryos (67,5%; n = 83, see **K**) showed strong expression of *Pt-fgf8* in the region around the migrating cumulus (indicated by the *Ets4* and pMad signal). (**J**) Ectodermal expression of *Pt-fgf8* in the germ-disc cells overlaying the cumulus. (**K**) Schematic drawing of germ-discs at late-stage 5, indicating the percentages of embryos that displayed a similar *Pt-fgf8* expression pattern (n = 83). Double *in situ* hybridisation showing *Pt-fgf8* expression in blue and the cumulus marker *Pt-Ets4* in orange (**D**, **E**, **G-I**). **C** and **J** show maximum intensity projections and orthogonal views of confocal scans of fluorescently labelled embryos (via pMad antibody staining and *in situ* hybridisation using fast red as a substrate). All embryos were co-stained with the nuclear dye DAPI or Sytox green. *Pt-fgf8* expression beyond stage 5 is depicted in Fig. S10.

to shift towards the rim of the germ-disc. At these stages, some embryos showed little (Figs. S7C, E, G, H) or patchy, salt and pepper like expression of *Pt-fgf8* (Fig. 4F e.g. Fig. S7I), others had a ring-like expression domain (Fig. 4G, Fig. S7 J-M) and few embryos showed no *Pt-fgf8* expression (Fig. S7F).

Importantly, during stage 5, *Pt-fgf8* expression was always switched off from the centre of the germ-disc (Fig. 4F–J, Figs. S7–S9).

In contrast to this dynamic and variable expression until mid-stage 5, we observed a very consistent feature of *Pt-fgf8* expression at late-stage 5. In all analysed embryos (n > 110) the cumulus reached the rim of the germ-disc at high levels of ectodermal *Pt-fgf8* expression (Fig. 4H–J, Figs. S8 and S9). Confocal sectioning of embryos revealed that fluorescently labelled *Pt-fgf8* transcripts were present in ectodermal, pMad positive, germ-disc cells (Fig. 4J). In the majority of embryos (67,5% see Fig. 4K), the ectodermal, *Pt-fgf8* expressing cells were directly anterior to the travelling cumulus cells (e.g. Fig. 4H).

Overall, *Pt-fgf8* showed a very stochastic and variable expression during germ-disc stages and most embryos had a unique *Pt-fgf8* expression pattern. Despite this, the very asymmetric expression of *Pt-fgf8* at late-stage 4 and the strong expression of *Pt-fgf8* at the final position of the cumulus at late-stage 5, combined with the observation that *Pt-FGFR1* as well as *Pt-dof* are expressed within the cells of the cumulus, create a setup of FGFR signalling components that are potentially recruited to guide the cumulus cells towards the rim of the germ-disc.

3.3. Possible ancestral function of FGFR-signalling in cumulus migration

As already mentioned above, the genomes of *P. tepidariorum* and *T. antipodiana* seemed to be missing the ortholog for *fgf17*. To see whether Fgf17 might have a role during cumulus migration in other spider species, we cloned *fgf17* and analysed its expression in *S. grossa* (a cobweb spider species, closely related to *P. tepidariorum*) and *A. geniculata* (a basally branching mygalomorph spider species). Live imaging of *S. grossa* embryos revealed that embryogenesis is very similar to *P. tepidariorum* embryogenesis (see Movie S4). Expression analysis revealed that *S. grossa fgf17* (*Sg-fgf17*) did not appear to be expressed at germ-disc stages (Fig. S11B). This was in contrast to *Sg-fgf8* that showed a similar and variable expression (see Fig. S11A), as was shown for *Pt-fgf8* in germ-disc stage *P. tepidariorum* embryos (e.g. Fig. 4). *A. geniculata fgf8* (*Ag-fgf8*) and *fgf17* (*Ag-fgf17*) showed both a variable expression pattern at stage 5 of embryogenesis and sometimes with enhanced expression in the region of the cumulus (Figs. S12G and H). Like in *P. tepidariorum*, also *Ag-FGFR1* (but not *Ag-FGFR2*) and *Ag-dof* was expressed in cells of the migrating cumulus (Figs. S12C–E). This analysis indicated that in basally branching spiders FGF signalling might also be involved in cumulus migration. For *fgf1* we could not detect any specific embryonic localisation of transcripts, neither in *P. tepidariorum* nor in *A. geniculata* (Fig. S12F, Fig. S13A, Fig. S14).

Supplementary data related to this article can be found at https://doi.org/10.1016/j.ydbio.2022.11.009.

3.4. The transcription factor Pt-Ets4 regulates expression of FGF signalling components in the cumulus

The primary thickening of stage 4 embryos is a cluster of gastrulating cells that enter the germ-disc via the blastopore (Akiyama-Oda and Oda, 2003; Hilbrant et al., 2012; Oda and Akiyama-Oda, 2008; Pechmann, 2016). In *P. tepidariorum*, around nine cells of the primary thickening contribute to the mesenchymal cell cluster of the migrating cumulus (Akiyama-Oda and Oda, 2003). We previously showed that the transcription factor *Pt-Ets4* is expressed in the cells of the primary thickening (see Fig. 5A) and in the migrating cumulus (Pechmann et al., 2017). We identified *Pt-Ets4* as an important factor for maintaining the cohesion of the cumulus cells and could show that *Pt-Ets4* is required to activate

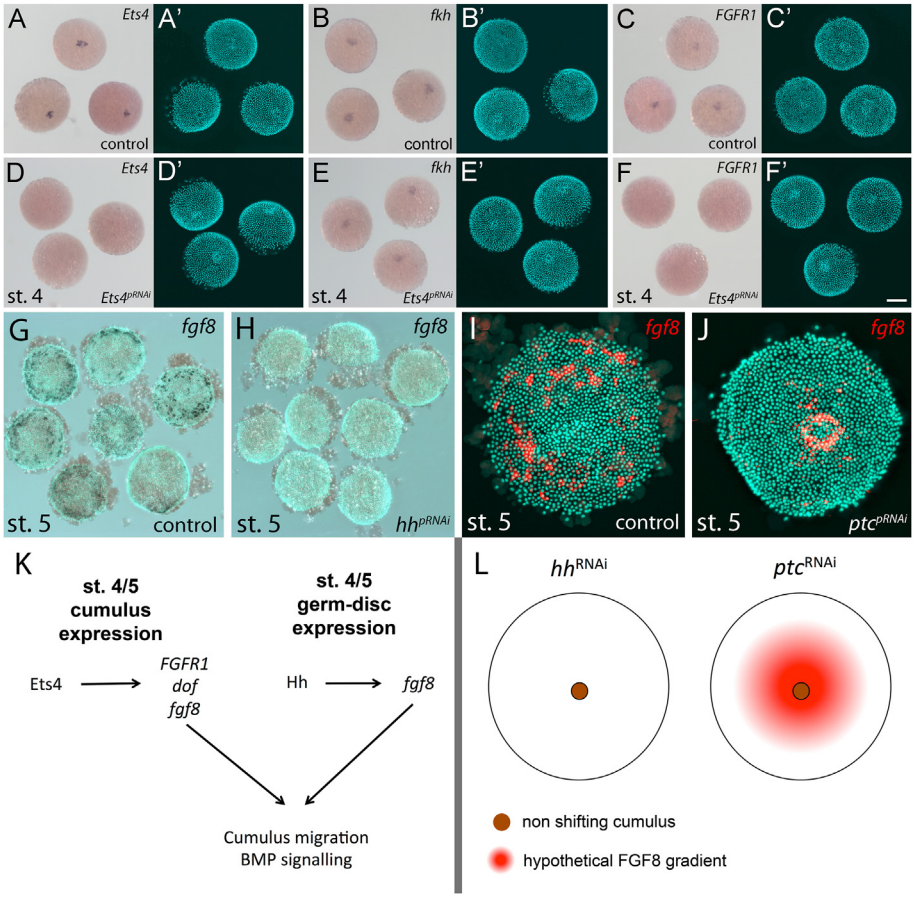

Fig. 5. Upstream and downstream of FGF signalling. (A-**F**) FGF signalling components were regulated by *Pt-Ets4* (compare to Table 1 and Figs. S5J and K). (**A, A′** and **D, D′**) *Pt-Ets4* expression in control and *Pt-Ets4* RNAi embryos. (**B, B′** and **E, E′**) Positive control. As shown before (Pechmann et al., 2017), *Pt-Ets4* was not affecting the expression of *Pt-fkh* in the cumulus. (**C, C′** and **F, F′**) The expression of *Pt-FGFR1* was absent in *Pt-Ets4* pRNAi embryos. Scale bar is 200 μm (**F′**). (**G-J**) Hedgehog signalling influenced *Pt-fgf8* expression in germ-disc embryos. *Pt-fgf8* expression was absent in *Pt-hh* RNAi embryos (**H**). Knockdown of the receptor *Pt-ptc* led to ectopic activation of Pt-*fgf8* in the centre of the germ-disc (**J**). (**K**) Simplified gene regulatory network (GRN) that is responsible for the regulation of components of the FGF signalling pathway in the cumulus and in the ectoderm of the germ-disc. (**L**) Top view on the germ-disc of stage 5 RNAi embryos. The brown circle indicates the cumulus that is not shifting in *hh* and *ptc* RNAi embryos. In the *ptc* RNAi embryo, hypothetical Fgf8 protein levels are indicated in red shading. The cumulus of strongly affected *hh* and *ptc* RNAi embryos does not shift because of the missing (in *hh* RNAi, see Fig. 5H) or the ectopic, central (in *ptc* RNAi, see Fig. 5J) expression of *fgf8*.

cumulus specific genes. Furthermore, ectopic expression of *Pt-Ets4* was able to induce cell delamination and migration (Pechmann et al., 2017).

To better understand the hierarchy of gene regulatory networks in the cumulus we evaluated genes with known cumulus expression in *Pt-Ets4* knockdowns. *Pt-fkh*, which was previously shown to be expressed in the primary thickening, was unaffected in *Pt-Ets4* knockdown embryos (Fig. 5B, E), indicating that *Pt-Ets4* does not activate the expression of *Pt-fkh*. However, when we surveyed *Pt-fgf8*, *Pt-FGFR1* and *Pt-dof* we found disruptions in their expression, suggesting that FGFR signalling is downstream of Ets4 activation. *Pt-FGFR1* expression was completely absent in *Pt-Ets4* RNAi embryos (Fig. 5 C, F) and the expression of *Pt-dof* was greatly reduced upon *Pt-Ets4* knockdown (Figs. S5J and K). In addition, we dissected the primary thickening from stage 4 *Pt-Ets4* pRNAi and control embryos, and performed differential expression analysis of genes being regulated by *Pt-Ets4*. This analysis confirmed that *Pt-FGFR1*, *Pt-dof*, and *Pt-fgf8* have significantly reduced expression levels in *Pt-Ets4* knockdown embryos (see Table 1).

3.5. Knockdown of Pt-fgf8 influences the activation of the BMP signalling pathway

As shown in previous studies, the down regulation of the Hedgehog (Hh) receptor Patched (*Pt-ptc*) inhibited cumulus migration (Akiyama-Oda and Oda, 2010; Pechmann et al., 2017). However, there was a fundamental difference between the *Pt-ptc* and the *Pt-fgf8* knockdown phenotype.

In wild type embryos, the shifting and Dpp secreting cumulus leads to the activation of the BMP signalling pathway at the periphery of the germ-disc. This leads to dorsal field formation, which is required to transform the radially symmetric germ-disc into a bilaterally symmetric germ-band. The cumulus cells of the *Pt-ptc* RNAi embryos are still able to activate the BMP signalling pathway in nearby ectodermal germ-disc cells (Akiyama-Oda and Oda, 2010). However, as the cumulus of *Pt-ptc* knockdown embryos was not shifting, the dorsal field was established in the centre of the germ-disc. An ectopic formation of the dorsal field in the

Table 1
Expression changes of FGF signalling components after pRNAi with dsRed (control) and *Ets4 in P. tepidariorum*. Stated are the TPM values (Transcripts Per Million) for all three replicates, the false discovery rate (FDR), and the Log2 fold expression change. Analysis performed with edgeR on the Degust platform.

gene	FDR	Log2 fold change	dsRed pRNAi #1	dsRed pRNAi #2	dsRed pRNAi #3	Ets4 pRNA #1	Ets4 pRNAi #2	Ets4 pRNAi #3
Ets4	3,80E-09	−3.98	161.599	196.816	241.265	2.20942	3.25887	26.740
fgf8	2,05E-02	−2.00	46.3583	80.273	56.327	6.65353	4.35487	29.179
Dof	1,48E-04	−4.29	9.30084	6.15884	10.958	0.238895	0.094327	0.471
fgfr1	1,59E-04	−3.27	9.56246	8.5299	15.184	0.82618	0.580557	1.184
fgfr2	1,00E+00	−0.22	2.48446	2.67093	2.650	2.5176	1.55443	1.477

centre of the germ-disc never occurred in *Pt-fgf8* RNAi embryos (Figs. 1–3, Movie S1 and Movie S2). This suggested to us that FGFR signalling is required to activate the BMP signalling pathway in stage 5 spider embryos.

To see at what level the FGFR signalling pathway was required to activate the BMP signalling pathway, we performed an *in situ* hybridisation to detect *Pt-dpp* transcripts and performed a pMad antibody staining to analyse BMP pathway activity in *Pt-fgf8* knockdown embryos (Fig. S15). This revealed that in the portion of *Pt-fgf8* pRNAi embryos that showed cumulus migration defects (23%; n = 59) the levels of *Pt-dpp* transcripts were virtually unchanged in comparison to *Pt-fgf8* pRNAi embryos that showed a normal shift of the cumulus cells during embryonic stage 5 (see Fig. S15). However, in *Pt-fgf8* pRNAi embryos lacking cumulus migration the pMad signal, which is an indicator for the activated BMP signalling pathway, was severely reduced in 14% of the analysed embryos (n = 139).

Furthermore, to check for cumulus formation defects, we analysed *Pt-fgf8* pRNAi embryos, derived from the same cocoon, for the expression of the cumulus marker *Pt-Ets4*. As *Pt-Ets4* expression was virtually unchanged in all analysed embryos (n = 72), we concluded that the formation of the cumulus was not affected by the downregulation of *Pt-fgf8* (see Fig. S15).

Overall, the experiment indicated that FGFR signalling is neither influencing the formation of the cumulus nor it is involved in the regulation of the expression of the BMP ligand *Pt-dpp*. Rather, FGFR signalling is required for the activation of the BMP signalling pathway downstream of Dpp.

3.6. *Pt-fgf8 expression is regulated via the Hh signalling pathway*

A genome wide search for genes being regulated by the Hh signalling pathway showed that *Pt-fgf8* expression levels were significantly altered upon *Pt-hh* and *Pt-ptc* RNAi (Akiyama-Oda and Oda, 2020). As our experiments indicate that *Pt-fgf8* might be an important factor controlling cumulus migration, we repeated the published *Pt-ptc* and *Pt-hh* knockdown experiments and analysed the expression of *Pt-fgf8* in stage 5 embryos. Our experiments confirmed the results by Akiyama-Oda and Oda and showed that *Pt-fgf8* transcripts are no longer detectable in *Pt-hh* RNAi embryos (Fig. 5G and H). In contrast, knockdown of *Pt-ptc* did lead to an ectopic, central activation of *Pt-fgf8* expression at stage 5 of embryonic development (Fig. 5I and J). As discussed below (see discussion and Fig. 5L) these results are in accordance with published cumulus migration defect phenotypes that were observed in *Pt-ptc* and *Pt-hh* knockdown embryos.

4. Discussion

During embryogenesis of most animals, BMP signalling is involved in setting up the dorsoventral (DV) body axis (reviewed in e.g. (De Robertis, 2008)). In spiders, the migrating cumulus is the source of this BMP signal that induces DV axis formation. In this arthropod system, the controlled localisation of the BMP signal (via local secretion of Dpp from cumulus cells) is necessary and sufficient to induce DV axis formation (Akiyama-Oda and Oda, 2006; Oda et al., 2020; Pechmann, 2020; Pechmann et al., 2017). The failure of cumulus migration, the loss of the cumulus or the loss of the BMP signal, all result in severe DV body axis patterning defects (this study (Akiyama-Oda and Oda, 2010, 2006; Pechmann, 2020; Pechmann et al., 2017)).

Here we show, that FGFR signalling is involved in cumulus migration in the spider *P. tepidariorum*. We provide evidence that FGFR signalling is regulated by the transcription factor Ets4 and via the Hh signalling pathway. Finally, we show that FGFR signalling is also involved in BMP signal transduction.

4.1. *FGFR signalling is involved in cumulus migration in spiders*

The observation that FGF receptor knockdowns (this study (Akiyama-Oda and Oda, 2010)) did not lead to any detectable cumulus migration phenotype and that the knockdowns of the ligand *Pt-fgf8* and the downstream factor *Pt-dof* only led to a phenotype in a subset of embryos (although *Pt-fgf8* transcript levels are greatly reduced and no longer detectable via *in situ* hybridisation, in almost all germ-disc stage embryos (see Fig. S16)) indicates that this FGFR signalling dependent cumulus migration is a robust process that is not easily perturbed by RNAi, at least in *P. tepidariorum*. It is very likely that small amounts of FGF ligand as well as remnants (or maternally provided) of FGF receptors are already sufficient to initiate normal cumulus migration and signalling. Nevertheless, the fact that we observed a similar FGF signalling phenotype for the ligand (*Pt-fgf8*) as well as for the downstream component (*Pt-dof*) revealed that FGFR signalling has a role in cumulus migration in the spider.

Our expression analysis clearly showed that in evolutionary younger spiders like *P. tepidariorum* as well as in the basally branching spider, like the tarantula *A. geniculata*, several components of the FGFR signalling pathway were expressed either in the germ-disc (*Pt-fgf8*, *Sg-fgf8*, *Ag-fgf8* and *Ag-fgf17*) or in the cumulus itself (*Pt-dof*, *Ag-dof*, *Pt-FGFR1*, *Ag-FGFR1*). This analysis suggested to us, that FGFR signalling is also involved in cumulus migration in basally branching spiders. Expression analysis of FGF components in other chelicerate species (e.g. Opiliones, scorpions, whip spiders, etc.) are required to show if cumulus migration via FGF signalling is a synapomorphic character of chelicerates.

Our phylogenetic and expression analysis of FGF ligands indicates that there might be variation in the recruitment of different FGFs during the embryogenesis of different spider species. As shown by our analysis, the genomes of *P. tepidariorum* as well as of *T. antipodiana* seem to lack an *fgf17* ortholog. However, within cobweb spiders, this loss of *fgf17* might be specific to *Parasteatoda* and not to cobweb spiders in general, as we could find *fgf17* in *S. grossa* (a closely related cobweb spider). As we could not detect any expression of *Sg-fgf17* during germ-disc stages, *Sg-fgf17* might not have a function that is related to cumulus migration. This contrasts with the expression of *Ag-fgf17* in the tarantula that showed a very similar pattern to *Ag-fgf8*. These results indicate that both, Fgf8 and Fgf17, might have a role during cumulus migration in basally branching spiders like *A. geniculata* but that this function is restricted to Fgf8 in higher spiders. In turn, this might have facilitated the independent loss of *fgf17* in spiders like *P. tepidariorum*.

4.2. *FGF signalling is controlled via Hh signalling and the transcription factor Ets4*

Our results on the regulation of *Pt-fgf8* expression within the germ-disc are in agreement with the results of a recent publication, which showed the genome-wide identification of the downstream targets of the Hh signalling pathway (Akiyama-Oda and Oda, 2020). In both, Akiyama-Oda and Oda (2020) and this study, *Pt-fgf8* was not detected in the cells of the germ-disc after *Pt-hh* pRNAi (Fig. 5H). Furthermore, like in our study, *Pt-fgf8* was ectopically activated in the central region of the germ-disc upon pRNAi of the negative regulator of the Hh signalling pathway *Pt-ptc* (Fig. 5J) (Akiyama-Oda and Oda, 2020).

Previously, we identified the transcription factor Ets4 as an important player for dorsoventral axis formation in *P. tepidariorum* (Pechmann et al., 2017). On the one hand, down-regulation of *Pt-Ets4* lead to the loss of the integrity of the cumulus cells. As a consequence, the cohesion of the cumulus cells was lost and therefore DV body axis formation was not initiated. On the other hand, ectopic expression of *Pt-Ets4* did lead to ectopic cell delamination and to an independent initiation of cell-migration of single cells. These results indicated that *Pt-Ets4* is an important player within the cumulus but is not sufficient on its own to

induce the formation of an ectopic cumulus. It is likely that a combination of several molecular factors is required to fully set up a functional cumulus. To get a better idea of how *Pt-Ets4* is regulating different processes within the cells of the cumulus, we performed an RNA-seq experiment and compared the expression profile of *Pt-Ets4* RNAi cumuli with those cumuli of control embryos. This analysis clearly showed that the early activation of several components of the FGF signalling pathway within the developing cumulus cells seems to be under the control of *Pt-Ets4* (Table 1). As FGF signalling is clearly involved in cell migration, this analysis indicates a link between *Pt-Ets4* and cumulus cell migration.

5. Conclusions and future directions

During early spider embryogenesis the cumulus shifts from the centre to the periphery of the radially symmetric germ-disc. It is still unclear if this is a completely stochastic process or if the cumulus is directed towards the rim of the disc via an unknown mechanism. Live imaging of cumulus migration in different spider species indicates that the movement of the cumulus towards the rim of the disc is relatively straight, once the cumulus has started to migrate (see Movie S1 and 2, e.g. (Akiyama-Oda and Oda, 2010; Chaw et al., 2007; Mittmann and Wolff, 2012; Wolff and Hilbrant, 2011)). This holds even true for very huge tarantula embryos (Pechmann, 2020). It was noted that in around 25% of wild type *P. tepidariorum* embryos, the cumulus is not perfectly centred within the germ-disc but is slightly asymmetrically positioned. However, even in these embryos the cumulus movement seems to not correlate with the positioning of the cumulus within the germ-disc and cumulus cells do not necessarily take the shortest distance to reach the rim of the disc (Akiyama-Oda and Oda, 2003). These observations indicate that an unknown mechanism might be responsible to give a direction to the shifting cumulus cells.

Although the expression of *Pt-fgf8* is highly variable in germ-disc stage *P. tepidariorum* embryos, we hypothesise that the stochastic and often very asymmetric expression of *Pt-fgf8* during stage 4 embryos (before cumulus migration, e.g. Fig. 4D and E) is be able to set up a short-term concentration gradient of Fgf8 protein across the germ-disc at early stage 4. As a result, this FGF gradient could be interpreted by the cumulus cells and could be responsible for the initial directional movement of the cumulus cells. Depending on the strength of this asymmetric or more uniform *Pt-fgf8* expression the hypothetical Fgf8 protein gradient could either be relatively steep or flatter.

Studies in other animal model systems were able to show that FGFs can act as a chemo-attractant (e.g. (Clark et al., 2011; Sato and Kornberg, 2002), reviewed in (Muha and Müller, 2013)). Our observation that *P. tepidariorum* cumulus cells, at late stage 5, always stop their migration at high levels of *Pt-fgf8* expression (Fig. 4H, I, J, K; Figs. S8 and S9) indicates that also in the spider Fgf8 might act as a chemo-attractant.

Unfortunately, we failed to regionally down-regulate (via embryonic RNAi) or over-activate *Pt-fgf8* expression (via embryonic capped mRNA injection) in the germ-disc of *P. tepidariorum* embryos. In the future, cell culture as well as bead transplantation experiments (Pechmann, 2020) could be useful to analyse if Fgf8 is indeed able to attract cumulus cells.

The strongest evidence that Fgf8 acts as a chemo attractant to guide cumulus cells, comes from the down regulation of Hh-signalling components and the subsequent changes in *Pt-fgf8* expression (see Fig. 5). As indicated in Fig. 5L, these differences in *Pt-fgf8* expression and the resulting putative differences in the Fgf8 protein gradients, might explain the observed alterations in cumulus migration (this study (Akiyama-Oda and Oda, 2020, 2010)). Briefly, in strongly affected *Pt-hh* as well as in *Pt-ptc* RNAi embryos cumulus migration was prevented (Akiyama-Oda and Oda, 2010). This loss of cumulus migration could be explained by the loss (in *Pt-hh* RNAi) or the ectopic central activation (in *Pt-ptc* RNAi) of *Pt-fgf8* expression. In the case of the loss of *Pt-fgf8* expression in *Pt-hh* RNAi embryos, cumulus attraction via *Pt-fgf8* is missing. As a result, cumulus migration is not initiated. In contrast, the ectopic central *Pt-fgf8* activation in *Pt-ptc* RNAi embryos would strongly attract and keep the cumulus cells in the middle of the germ-disc (Fig. 5L). Our expression analysis indicates that the clearance of *Pt-fgf8* transcripts from the centre of the stage 5 germ-disc, is an important aspect of the dynamic *Pt-fgf8* expression. This observation further supports the idea that the central ectopic expression of *Pt-fgf8* in *Pt-ptc* knockdown embryos prevented the cumulus from shifting.

In *P. tepidariorum*, Hh signalling is involved in patterning the anteroposterior axis of the germ-disc (Akiyama-Oda and Oda, 2010, 2020). This leads to the suggestion that Hh signalling might set up a positional value gradient across the germ-disc and that the cumulus cells move down along this emerging positional value gradient (Akiyama-Oda and Oda, 2010). Hh protein in vertebrate embryos might be able to travel a distance of around 300 μm, which is very similar to the radius of *P. tepidariorum* germ-disc stage embryos (Akiyama-Oda and Oda, 2010; Lewis et al., 2001). However, the size of spider eggs and embryos is very diverse. In *A. geniculata* the radius of the germ-disc is already around 1 mm (Pechmann, 2020) and the embryos of this species are not the biggest amongst Mygalomorphae. For this reason, it is very likely that a different mechanism is involved in guiding the cumulus cells towards the rim of the germ-disc. The observation that in many embryos, strong *Pt-fgf8* expression was directly anterior to the migrating cumulus cells (e.g. Fig. 4H, K, several embryos in Fig. S8) indicate a self-activating system, in which the cumulus on its own is driving the activation of a chemo-attractant in a posterior (centre of the germ-disc) to anterior (rim of the germ-disc) direction. While the cumulus shifts underneath the germ-disc, the cumulus mechanically pushes the ectoderm upwards (Akiyama-Oda and Oda, 2010). This cumulus driven bulging might induce mechanical stress in the overlaying ectoderm, which in turn could trigger the further activation of *fgf8* expression in front of the migrating cumulus. It was shown that mechanically induced stretching or compression of cells is able to induce receptor activation and gene expression, including fibroblast growth factor receptors and ligands (e.g. (Kinoshita et al., 2020; Li and Hughes-Fulford, 2006)). A self-enhancing system would not depend on a stable and long lasting long-range morphogen gradient. Therefore, it might be functional in any spider embryo, regardless of the size of the germ-disc.

Alternative mechanisms could also lead to the local enhancement of FGFs within certain regions of the germ-disc, and this might then lead to the local attraction of cumulus cells. In zebrafish lateral line formation, it was shown that apical constriction leads to the formation of microlumen, which are in the centre of rosette-like structures. These structures are responsible to trap secreted FGFs and are able to increase signalling responses and the coordination of migratory cell behaviour (reviewed in (Chan et al., 2017), original article (Durdu et al., 2014)). So far, it is not known whether similar structures exist in spider embryos.

Our results indicate that *Pt-fgf8* is also required to activate the BMP signalling pathway in ectodermal germ-disc cells overlaying the cells of the cumulus. In wild-type embryos, this activation is crucial to induce the dorsal field at the rim of the disc. This in turn is required to break the radially symmetry of the germ-disc (e.g. (Akiyama-Oda and Oda, 2006; Oda and Akiyama-Oda, 2008)).

The performed analysis indicates that the involvement of *Pt-Fgf8* in activating the BMP signalling pathway is very likely not on the level of ligand (*Pt-dpp* expression was not affected) activation but seems to be downstream of receptor activation. Future studies, like a genome wide search of target genes of FGFR signalling might help to understand, if FGFs are really required to activate the BMP signalling pathway or if other mechanisms are causing the observed phenotype. In *Drosophila* it was shown that FGF signalling is involved in cytoneme formation (e.g. (Du et al., 2018)). Also in *P. tepidariorum* germ-disc embryos cytoplasmic cytoneme like structures that were projecting from the cumulus towards the germ-disc epithelium could be identified (Akiyama-Oda and Oda, 2003). Cytonemes are known to be important players in the BMP signalling pathway (Kornberg, 2017; Kornberg and Roy, 2014; Zhang and Scholpp, 2019). For this reason, missing cytonemes might be the reason

that strongly affected *Pt-fgf8* knockdown embryos are lacking an active BMP signalling pathway.

Disclaimer

The funders had no role in study design, data collection and analysis, decision to publish or preparation of the manuscript.

Funding

This work has been funded by the Deutsche Forschungsgemeinschaft (DFG grant PE 2075/1-2 and PE 2075/3–1 to M.P. and DFG grant SCHI 1365/2–1 to P.S.).

Authors' contributions

M.P. designed the study, performed RNAi experiments and the phylogenetic analysis and wrote the paper. R.W. performed the RNA sequencing experiment, performed parts of the molecular and bioinformatics analysis and commented on the manuscript. P.S. performed the initial bioinformatics analysis of the RNA seq. data and commented on the manuscript. L.K. performed *in situ* analysis in *A. geniculata* and commented on the manuscript. D.J.L performed the synteny analysis and commented on the manuscript. All authors gave final approval for publication.

Declaration of competing interest

We declare we have no competing interests.

Data availability

Data will be made available on request.

Acknowledgements

We thank Siegfried Roth for commenting on the manuscript.

We would also like to thank two anonymous reviewers for their helpful comments on the manuscript.

Appendix A. Supplementary data

Supplementary data to this article can be found online at https://doi.org/10.1016/j.ydbio.2022.11.009.

References

Akiyama-Oda, Y., Oda, H., 2020. Hedgehog signaling controls segmentation dynamics and diversity via msx1 in a spider embryo. Sci. Adv. 6. https://doi.org/10.1126/sciadv.aba7261 eaba7261.

Akiyama-Oda, Y., Oda, H., 2010. Cell migration that orients the dorsoventral axis is coordinated with anteroposterior patterning mediated by Hedgehog signaling in the early spider embryo. Development 137, 1263–1273. https://doi.org/10.1242/dev.045625.

Akiyama-Oda, Y., Oda, H., 2006. Axis specification in the spider embryo: dpp is required for radial-to-axial symmetry transformation and sog for ventral patterning. Development 133, 2347–2357. https://doi.org/10.1242/dev.02400.

Akiyama-Oda, Y., Oda, H., 2003. Early patterning of the spider embryo: a cluster of mesenchymal cells at the cumulus produces Dpp signals received by germ disc epithelial cells. Development 130, 1735–1747. https://doi.org/10.1242/dev.00390.

Altschul, S.F., Gish, W., Miller, W., Myers, E.W., Lipman, D.J., 1990. Basic local alignment search tool. J. Mol. Biol. 215, 403–410. https://doi.org/10.1016/S0022-2836(05)80360-2.

Beermann, A., Schröder, R., 2008. Sites of Fgf signalling and perception during embryogenesis of the beetle Tribolium castaneum. Dev. Gene. Evol. 218, 153–167. https://doi.org/10.1007/s00427-007-0192-x.

Benton, M.A., Pechmann, M., Frey, N., Stappert, D., Conrads, K.H., Chen, Y.-T., Stamataki, E., Pavlopoulos, A., Roth, S., 2016. Toll genes have an ancestral role in Axis elongation. Curr. Biol. 26, 1609–1615. https://doi.org/10.1016/j.cub.2016.04.055.

Borland, C.Z., Schutzman, J.L., Stern, M.J., 2001. Fibroblast growth factor signaling in Caenorhabditis elegans. Bioessays 23, 1120–1130. https://doi.org/10.1002/bies.10007.

Bray, N.L., Pimentel, H., Melsted, P., Pachter, L., 2016. Near-optimal probabilistic RNA-seq quantification. Nat. Biotechnol. 34, 525–527. https://doi.org/10.1038/nbt.3519.

Buchfink, B., Reuter, K., Drost, H.-G., 2021. Sensitive protein alignments at tree-of-life scale using DIAMOND. Nat. Methods 18, 366–368. https://doi.org/10.1038/s41592-021-01101-x.

Burdine, R.D., Branda, C.S., Stern, M.J., 1998. EGL-17(FGF) expression coordinates the attraction of the migrating sex myoblasts with vulval induction in C. elegans. Development 125, 1083–1093.

Capella-Gutiérrez, S., Silla-Martínez, J.M., Gabaldón, T., 2009. trimAl: a tool for automated alignment trimming in large-scale phylogenetic analyses. Bioinformatics 25, 1972–1973. https://doi.org/10.1093/bioinformatics/btp348.

Chan, C.J., Heisenberg, C.-P., Hiiragi, T., 2017. Coordination of morphogenesis and cell-fate specification in development. Curr. Biol. 27, R1024–R1035. https://doi.org/10.1016/j.cub.2017.07.010.

Chaw, R.C., Vance, E., Black, S.D., 2007. Gastrulation in the spider Zygiella x-notata involves three distinct phases of cell internalization. Dev. Dynam. 236, 3484–3495. https://doi.org/10.1002/dvdy.21371.

Chen, S., Zhou, Y., Chen, Y., Gu, J., 2018. fastp: an ultra-fast all-in-one FASTQ preprocessor. Bioinformatics 34, i884–i890. https://doi.org/10.1093/bioinformatics/bty560.

Clark, I.B.N., Muha, V., Klingseisen, A., Leptin, M., Müller, H.-A.J., 2011. Fibroblast growth factor signalling controls successive cell behaviours during mesoderm layer formation in Drosophila. Development 138, 2705–2715. https://doi.org/10.1242/dev.060277.

De Robertis, E.M., 2008. Evo-devo: variations on ancestral themes. Cell 132, 185–195. https://doi.org/10.1016/j.cell.2008.01.003.

Dereeper, A., Guignon, V., Blanc, G., Audic, S., Buffet, S., Chevenet, F., Dufayard, J.-F., Guindon, S., Lefort, V., Lescot, M., Claverie, J.-M., Gascuel, O., 2008. Phylogeny.fr: robust phylogenetic analysis for the non-specialist. Nucleic Acids Res. 36, W465–W469. https://doi.org/10.1093/nar/gkn180.

Dorey, K., Amaya, E., 2010. FGF signalling: diverse roles during early vertebrate embryogenesis. Development 137, 3731–3742. https://doi.org/10.1242/dev.037689.

Du, L., Sohr, A., Yan, G., Roy, S., 2018. Feedback regulation of cytoneme-mediated transport shapes a tissue-specific FGF morphogen gradient. Elife 7, e38137. https://doi.org/10.7554/eLife.38137.

Durdu, S., Iskar, M., Revenu, C., Schieber, N., Kunze, A., Bork, P., Schwab, Y., Gilmour, D., 2014. Luminal signalling links cell communication to tissue architecture during organogenesis. Nature 515, 120–124. https://doi.org/10.1038/nature13852.

Edgar, R.C., 2004. MUSCLE: multiple sequence alignment with high accuracy and high throughput. Nucleic Acids Res. 32, 1792–1797. https://doi.org/10.1093/nar/gkh340.

Escuer, P., Pisarenco, V.A., Fernández-Ruiz, A.A., Vizueta, J., Sánchez-Herrero, J.F., Arnedo, M.A., Sánchez-Gracia, A., Rozas, J., 2022. The chromosome-scale assembly of the Canary Islands endemic spider Dysdera silvatica (Arachnida, Araneae) sheds light on the origin and genome structure of chemoreceptor gene families in chelicerates. Mol Ecol Resour 22, 375–390. https://doi.org/10.1111/1755-0998.13471.

Fan, Z., Yuan, T., Liu, P., Wang, L.-Y., Jin, J.-F., Zhang, F., Zhang, Z.-S., 2021. A chromosome-level genome of the spider Trichonephila antipodiana reveals the genetic basis of its polyphagy and evidence of an ancient whole-genome duplication event. GigaScience 10. https://doi.org/10.1093/gigascience/giab016 giab016.

Hilbrant, M., Damen, W.G.M., McGregor, A.P., 2012. Evolutionary crossroads in developmental biology: the spider Parasteatoda tepidariorum. Development 139, 2655–2662. https://doi.org/10.1242/dev.078204.

Holm, Å., 1952. Experimentelle Untersuchungen über die Entwicklung und Entwicklungsphysiologie des Spinnenembryos. Almqvist & Wiksells, Uppsala.

Kinoshita, N., Hashimoto, Y., Yasue, N., Suzuki, M., Cristea, I.M., Ueno, N., 2020. Mechanical stress regulates epithelial tissue integrity and stiffness through the FGFR/Erk2 signaling pathway during embryogenesis. Cell Rep. 30, 3875–3888. https://doi.org/10.1016/j.celrep.2020.02.074 e3.

Kornberg, T.B., 2017. Distributing signaling proteins in space and time: the province of cytonemes. Curr. Opin. Genet. Dev. 45, 22–27. https://doi.org/10.1016/j.gde.2017.02.010.

Kornberg, T.B., Roy, S., 2014. Cytonemes as specialized signaling filopodia. Development 141, 729–736. https://doi.org/10.1242/dev.086223.

Krzywinski, M., Schein, J., Birol, I., Connors, J., Gascoyne, R., Horsman, D., Jones, S.J., Marra, M.A., 2009. Circos: an information aesthetic for comparative genomics. Genome Res. 19, 1639–1645. https://doi.org/10.1101/gr.092759.109.

Lewis, P.M., Dunn, M.P., McMahon, J.A., Logan, M., Martin, J.F., St-Jacques, B., McMahon, A.P., 2001. Cholesterol modification of sonic hedgehog is required for long-range signaling activity and effective modulation of signaling by Ptc1. Cell 105, 599–612. https://doi.org/10.1016/s0092-8674(01)00369-5.

Li, C.-F., Hughes-Fulford, M., 2006. Fibroblast growth factor-2 is an immediate-early gene induced by mechanical stress in osteogenic cells. J. Bone Miner. Res. 21, 946–955. https://doi.org/10.1359/jbmr.060309.

Lo, T.-W., Bennett, D.C., Goodman, S.J., Stern, M.J., 2010. Caenorhabditis elegans fibroblast growth factor receptor signaling can occur independently of the multi-substrate adaptor FRS2. Genetics 185, 537–547. https://doi.org/10.1534/genetics.109.113373.

McGregor, A.P., Pechmann, M., Schwager, E.E., Feitosa, N.M., Kruck, S., Aranda, M., Damen, W.G.M., 2008. Wnt8 is required for growth-zone establishment and

development of opisthosomal segments in a spider. Curr. Biol. 18, 1619–1623. https://doi.org/10.1016/j.cub.2008.08.045.
Mittmann, B., Wolff, C., 2012. Embryonic development and staging of the cobweb spider Parasteatoda tepidariorum C. L. Koch, 1841 (syn.: Achaearanea tepidariorum; Araneomorphae; Theridiidae). Dev. Gene. Evol. 222, 189–216. https://doi.org/10.1007/s00427-012-0401-0.
Muha, V., Müller, H.-A.J., 2013. Functions and mechanisms of fibroblast growth factor (FGF) signalling in Drosophila melanogaster. Int. J. Mol. Sci. 14, 5920–5937. https://doi.org/10.3390/ijms14035920.
Oda, H., Akiyama-Oda, Y., 2008. Differing strategies for forming the arthropod body plan: lessons from Dpp, Sog and Delta in the fly Drosophila and spider Achaearanea. Dev. Growth Differ. 50, 203–214. https://doi.org/10.1111/j.1440-169X.2008.00998.x.
Oda, H., Iwasaki-Yokozawa, S., Usui, T., Akiyama-Oda, Y., 2020. Experimental duplication of bilaterian body axes in spider embryos: holm's organizer and self-regulation of embryonic fields. Dev. Gene. Evol. 230, 49–63. https://doi.org/10.1007/s00427-019-00631-x.
Pechmann, M., 2020. Embryonic development and secondary axis induction in the Brazilian white knee tarantula Acanthoscurria geniculata, C. L. Koch, 1841 (Araneae; Mygalomorphae; Theraphosidae). Dev. Gene. Evol. 230, 75–94. https://doi.org/10.1007/s00427-020-00653-w.
Pechmann, M., 2016. Formation of the germ-disc in spider embryos by a condensation-like mechanism. Front. Zool. 13, 35. https://doi.org/10.1186/s12983-016-0166-9.
Pechmann, M., Benton, M.A., Kenny, N.J., Posnien, N., Roth, S., 2017. A novel role for Ets4 in axis specification and cell migration in the spider Parasteatoda tepidariorum. Elife 6. https://doi.org/10.7554/eLife.27590.
Pechmann, M., McGregor, A.P., Schwager, E.E., Feitosa, N.M., Damen, W.G.M., 2009. Dynamic gene expression is required for anterior regionalization in a spider. Proc. Natl. Acad. Sci. U.S.A. 106, 1468–1472. https://doi.org/10.1073/pnas.0811150106.
Popovici, C., Roubin, R., Coulier, F., Birnbaum, D., 2005. An evolutionary history of the FGF superfamily. Bioessays 27, 849–857. https://doi.org/10.1002/bies.20261.
Posnien, N., Zeng, V., Schwager, E.E., Pechmann, M., Hilbrant, M., Keefe, J.D., Damen, W.G.M., Prpic, N.-M., McGregor, A.P., Extavour, C.G., 2014. A comprehensive reference transcriptome resource for the common house spider Parasteatoda tepidariorum. PLoS One 9, e104885. https://doi.org/10.1371/journal.pone.0104885.
Prpic, N.-M., Schoppmeier, M., Damen, W.G.M., 2008. Whole-Mount in situ hybridization of spider embryos. Cold Spring Harb. Protoc. 2008. https://doi.org/10.1101/pdb.prot5068 pdb.prot5068.
Sato, M., Kornberg, T.B., 2002. FGF is an essential mitogen and chemoattractant for the air sacs of the Drosophila tracheal system. Dev. Cell 3, 195–207. https://doi.org/10.1016/S1534-5807(02)00202-2.
Schindelin, J., Arganda-Carreras, I., Frise, E., Kaynig, V., Longair, M., Pietzsch, T., Preibisch, S., Rueden, C., Saalfeld, S., Schmid, B., Tinevez, J.-Y., White, D.J., Hartenstein, V., Eliceiri, K., Tomancak, P., Cardona, A., 2012. Fiji: an open-source platform for biological-image analysis. Nat. Methods 9, 676–682. https://doi.org/10.1038/nmeth.2019.
Schwager, E.E., Schönauer, A., Leite, D.J., Sharma, P.P., McGregor, A.P., 2015. Chelicerata. In: Wanninger, A. (Ed.), Evolutionary Developmental Biology of Invertebrates 3. Springer Vienna, pp. 99–139. https://doi.org/10.1007/978-3-7091-1865-8_5.
Schwager, E.E., Sharma, P.P., Clarke, T., Leite, D.J., Wierschin, T., Pechmann, M., Akiyama-Oda, Y., Esposito, L., Bechsgaard, J., Bilde, T., Buffry, A.D., Chao, H., Dinh, H., Doddapaneni, H., Dugan, S., Eibner, C., Extavour, C.G., Funch, P., Garb, J., Gonzalez, L.B., Gonzalez, V.L., Griffiths-Jones, S., Han, Y., Hayashi, C., Hilbrant, M., Hughes, D.S.T., Janssen, R., Lee, S.L., Maeso, I., Murali, S.C., Muzny, D.M., Nunes da Fonseca, R., Paese, C.L.B., Qu, J., Ronshaugen, M., Schomburg, C., Schönauer, A., Stollewerk, A., Torres-Oliva, M., Turetzek, N., Vanthournout, B., Werren, J.H., Wolff, C., Worley, K.C., Bucher, G., Gibbs, R.A., Coddington, J., Oda, H., Stanke, M., Ayoub, N.A., Prpic, N.-M., Flot, J.-F., Posnien, N., Richards, S., McGregor, A.P., 2017. The house spider genome reveals an ancient whole-genome duplication during arachnid evolution. BMC Biol. 15, 62. https://doi.org/10.1186/s12915-017-0399-x.
Sharma, R., Beer, K., Iwanov, K., Schmöhl, F., Beckmann, P.I., Schröder, R., 2015. The single fgf receptor gene in the beetle Tribolium castaneum codes for two isoforms that integrate FGF8- and Branchless-dependent signals. Dev. Biol. 402, 264–275. https://doi.org/10.1016/j.ydbio.2015.04.001.
Sharma, R., Beermann, A., Schröder, R., 2013. FGF signalling controls anterior extraembryonic and embryonic fate in the beetle Tribolium. Dev. Biol. 381, 121–133. https://doi.org/10.1016/j.ydbio.2013.05.031.
Sheffer, M.M., Hoppe, A., Krehenwinkel, H., Uhl, G., Kuss, A.W., Jensen, L., Jensen, C., Gillespie, R.G., Hoff, K.J., Prost, S., 2021. Chromosome-level reference genome of the European wasp spider Argiope bruennichi: a resource for studies on range expansion and evolutionary adaptation. GigaScience 10. https://doi.org/10.1093/gigascience/giaa148 giaa148.
Sun, X., Meyers, E.N., Lewandoski, M., Martin, G.R., 1999. Targeted disruption of Fgf8 causes failure of cell migration in the gastrulating mouse embryo. Genes Dev. 13, 1834–1846. https://doi.org/10.1101/gad.13.14.1834.
Thurmond, J., Goodman, J.L., Strelets, V.B., Attrill, H., Gramates, L.S., Marygold, S.J., Matthews, B.B., Millburn, G., Antonazzo, G., Trovisco, V., Kaufman, T.C., Calvi, B.R., FlyBase Consortium, 2019. FlyBase 2.0: the next generation. Nucleic Acids Res. 47, D759–D765. https://doi.org/10.1093/nar/gky1003.
Wang, Y., Tang, H., Debarry, J.D., Tan, X., Li, J., Wang, X., Lee, T., Jin, H., Marler, B., Guo, H., Kissinger, J.C., Paterson, A.H., 2012. MCScanX: a toolkit for detection and evolutionary analysis of gene synteny and collinearity. Nucleic Acids Res. 40, e49. https://doi.org/10.1093/nar/gkr1293.
Whelan, S., Goldman, N., 2001. A general empirical model of protein evolution derived from multiple protein families using a maximum-likelihood approach. Mol. Biol. Evol. 18, 691–699.
Wolff, C., Hilbrant, M., 2011. The embryonic development of the central American wandering spider Cupiennius salei. Front. Zool. 8, 15. https://doi.org/10.1186/1742-9994-8-15.
Xie, Y., Su, N., Yang, J., Tan, Q., Huang, S., Jin, M., Ni, Z., Zhang, B., Zhang, D., Luo, F., Chen, H., Sun, X., Feng, J.Q., Qi, H., Chen, L., 2020. FGF/FGFR signaling in health and disease. Signal Transduct. Targeted Ther. 5, 181. https://doi.org/10.1038/s41392-020-00222-7.
Zhang, C., Scholpp, S., 2019. Cytonemes in development. Current Opinion in Genetics & Development, Developmental mechanisms, patterning and evolution 57, 25–30. https://doi.org/10.1016/j.gde.2019.06.005.